A Half–Reaction Alternative to Water Oxidation: Chloride Oxidation to Chlorine Catalyzed by Silver Ion

4 AUTHORS, INCLUDING:

Jialei Du
Tongji University
4 PUBLICATIONS **10** CITATIONS

SEE PROFILE

Chuncheng Chen
Chinese Academy of Sciences
111 PUBLICATIONS **5,375** CITATIONS

SEE PROFILE

A Half-Reaction Alternative to Water Oxidation: Chloride Oxidation to Chlorine Catalyzed by Silver Ion

Jialei Du,[†] Zuofeng Chen,*,[†] Chuncheng Chen,*,[‡] and Thomas J. Meyer[§]

[†]Shanghai Key Lab of Chemical Assessment and Sustainability, Department of Chemistry, Tongji University, Shanghai 200092, China
[‡]Key Laboratory of Photochemistry, Institute of Chemistry, Chinese Academy of Sciences, Beijing 100190, China
[§]Department of Chemistry, University of North Carolina at Chapel Hill, Chapel Hill, North Carolina 27599, United States

S *Supporting Information*

ABSTRACT: Chloride oxidation to chlorine is a potential alternative to water oxidation to oxygen as a solar fuels half-reaction. Ag(I) is potentially an oxidative catalyst but is inhibited by the high potentials for accessing the Ag(II/I) and Ag(III/II) couples. We report here that the complex ions $AgCl_2^-$ and $AgCl_3^{2-}$ form in concentrated Cl^- solutions, avoiding AgCl precipitation and providing access to the higher oxidation states by delocalizing the oxidative charge over the Cl^- ligands. Catalysis is homogeneous and occurs at high rates and low overpotentials (10 mV at the onset) with μM Ag(I). Catalysis is enhanced in D_2O as solvent, with a significant H_2O/D_2O inverse kinetic isotope effect of 0.25. The results of computational studies suggest that Cl^- oxidation occurs by $1e^-$ oxidation of $AgCl_3^{2-}$ to $AgCl_3^-$ at a decreased potential, followed by Cl^- coordination, presumably to form $AgCl_4^{2-}$ as an intermediate. Adding a second Cl^- results in "redox potential leveling", with further oxidation to $\{AgCl_2(Cl_2)\}^-$ followed by Cl_2 release.
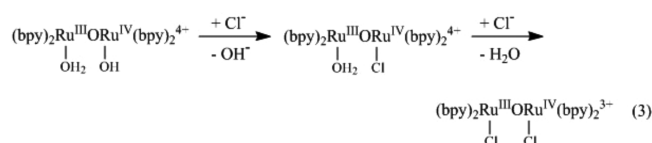
Water oxidation plays a key role in plant photosynthesis. It is also the "other" half-reaction in schemes of solar fuels, providing redox equivalents and protons for carrying out H^+ reduction to hydrogen or CO_2 reduction to a reduced form of carbon.[1] However, water oxidation to oxygen is both energetically and mechanistically demanding, requiring loss of $4e^-$ and $4H^+$ from two H_2O molecules with concomitant formation of an O---O bond. These demands lead to mechanistic complexity and, typically, slow kinetics and high overpotentials. Finding alternatives to this half-reaction could open the door to more efficient approaches to solar energy conversion.

Chloride oxidation to chlorine/hypochlorite is a potential alternative to H_2O oxidation to O_2. Cl^- is a major component of seawater. Seawater is 97% of Earth's water supply and contains >3% by weight NaCl (550 mM). Cl^- oxidation is 45% less demanding energetically, with $\Delta G° = 2.72$ eV in eq 1, compared to $\Delta G° = 4.92$ eV for H_2O oxidation in eq 2. In a photoelectrochemical application, there is a 2-photon requirement for Cl^- oxidation to Cl_2, compared to a 4-photon requirement for H_2O oxidation to O_2. As shown in the $E_{1/2}$–pH plot in the Supporting Information (SI), Figure S1, although $E°$ for the Cl_2/Cl^- couple (1.36 V vs NHE) is 130 mV higher than $E°$ for the O_2/H_2O couple (1.23 V), Cl^- oxidation to Cl_2 has the advantage of avoiding a high-energy peroxide intermediate

with $E°(O_2/H_2O_2) = 1.78$ V. Cl^- oxidation to Cl_2 may also be less complicated mechanistically because of the $2e^-$ requirement without a proton demand.

$$2Cl^- \rightarrow Cl_2 + 2e^-, \quad E° = 1.36 \text{ V} \tag{1}$$

$$2H_2O \rightarrow O_2 + 4H^+ + 4e^-, \quad E° = 1.23 \text{ V} \tag{2}$$
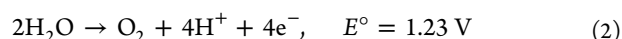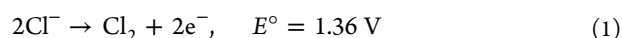
Cl^- oxidation to Cl_2 is carried out in the chlor-alkali process.[2] In this process, corrosion-resistant titania electrodes coated with RuO_2 or IrO_2 are used as the dimensionally stable anode (DSA). These metals are neither abundant nor inexpensive; they also tend to deactivate by surface poisoning or aggregation.[3] Homogeneous catalysts are more amenable to spectroscopic, physicochemical, and mechanistic investigation and thus more readily optimized. Electrocatalytic oxidation of Cl^- to Cl_2 by polypyridine Ru–aqua complexes,[4] their structurally related polymer derivatives,[5] or ferrocene in micellar media[6] has been reported. Ru–aqua catalyst activation in this case is based on a series of closely spaced, proton-coupled electron-transfer oxidations to give high-oxidation-state oxo forms. However, catalytic currents typically decrease with time due to Cl^- substitution for H_2O, eq 3.[4]

$$(bpy)_2Ru^{III}ORu^{IV}(bpy)_2^{4-} \xrightarrow[-OH^-]{+Cl^-} (bpy)_2Ru^{III}ORu^{IV}(bpy)_2^{4-} \xrightarrow[-H_2O]{+Cl^-}$$
$$\begin{matrix} | & | \\ OH_2 & OH \end{matrix} \qquad \begin{matrix} | & | \\ OH_2 & Cl \end{matrix}$$

$$(bpy)_2Ru^{III}ORu^{IV}(bpy)_2^{3-} \tag{3}$$
$$\begin{matrix} | & | \\ Cl & Cl \end{matrix}$$

Ag(I) has both a well-defined coordination chemistry and an extensive redox chemistry based on reduction to Ag(0) and oxidation to Ag(II) and/or Ag(III). Ag(II) is a strong oxidant, with $E°(Ag^{2+/+}) = 1.98$ V, eq 4. It is available by anodic oxidation of Ag(I) but is stable only in highly acidic solutions, e.g., 10 M HNO_3. With this limitation, most applications of the Ag(II/I) couple have come in mediated electrochemical oxidations in destructing organics.[7] Although invoked less commonly, there is precedence for involvement of more highly oxidizing Ag(III).[8]

$$Ag^+ - e^- \rightarrow Ag^{2+}, \quad E° = 1.98 \text{ V} \tag{4}$$
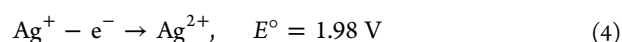
Here we report that, in concentrated Cl^- solutions, Ag(I) is highly active as a homogeneous catalyst for Cl^- oxidation to Cl_2. Under the experimental conditions used, Cl^- coordination

A

avoids precipitation of Ag(I) as AgCl and lowers redox potentials by delocalizing acceptor orbitals over the resulting complexes. Catalytic performance is impressive, with oxidation occurring at high rates and low overpotentials, even with μM Ag(I).

Initially, Ag(I) catalysis of H_2O oxidation without added Cl^- was investigated as a background reaction. H_2O oxidation electrocatalysis is impressive at pH 2, Figure S2, but the onset potential ($E_{onset} \approx 1.90$ V) during the forward scan is high, with an overpotential ~790 mV for H_2O oxidation, due to the high potential for accessing the Ag(II/I) couple. Similar phenomena were observed at pH 7, with $E_{onset} = 1.55$ V and a decreased reactivity, Figure S3. The shift in E_{onset} tracks the pH dependence of the $4e^-/4H^+$ O_2/H_2O couple and, presumably, the pH dependence of a higher oxidation state Ag(II/I) couple. Figures S4 and S5 present evidence for a surface precipitate during electrolyses under these conditions. It points to H_2O oxidation catalysis activated by oxidation of Ag(I) to Ag(II) with decomposition to precipitate an active surface film, Ag_2O, and oxidation of the surface oxide leading to O_2 evolution.[9]

Under catalytic conditions with 30 equiv of added Ce(IV) in 0.1 or 1 M HNO_3 containing 10−100 μM Ag(I), monitoring with an oxygen probe failed to detect O_2 as a product over 30 min. Given the potentials for the Ag(II/I) and Ce(IV/III) couples, with $E°(Ce^{4+/3+}) = 1.50$ V in 0.1 M HNO_3 and 1.61 V in 1.0 M HNO_3,[10] the low steady-state [Ag(II)] under these conditions greatly inhibits the rate of H_2O oxidation.

In H_2O, AgCl is poorly soluble, with $K_{sp} = 1.77 \times 10^{-10}$ at 298 K. However, in aqueous solutions with high [Cl^-], AgCl is solubilized by forming Cl^- complexes.[11] In this study, the solubility of Ag(I) as a function of added NaCl was determined by monitoring the surface plasmon resonance absorption of precipitated AgCl nanoparticles/nanoclusters. As shown in Figure S6, Ag(I) solubility is exponentially dependent on [Cl^-], consistent with the literature.[11a]

Figure 1A shows cyclic voltammograms (CVs) at a glassy carbon (GC) electrode (0.071 cm²) in aqueous solution 1 M in NaCl in 0.1 M HNO_3 (pH 1) with added Ag(I). Adding Ag(I) results in a remarkable catalytic current enhancement. There is direct evidence for oxidation of Cl^- to Cl_2 by the appearance of a reductive Cl_2-to-Cl^- wave at $E_{p,c} = 0.93$ V.[4] The E_{onset} value for Cl^- oxidation is ~1.37 V, near the thermodynamic potential for the Cl^-/Cl_2 couple, 1.36 V. This value is remarkably lower than $E°(Ag^{2+/+}) = 1.98$ V, with a ~600 mV shift to negative potential.

As shown in the Figure 1A inset, the catalytic current increases linearly with added Ag(I), with the dependence saturated at 80 μM, above which Ag(I) becomes insoluble. The linear relationship between the catalytic current and [Ag(I)] suggests

a single-site mechanism for Ag(I) catalysis of Cl^- oxidation. At pH 7, catalytic current enhancements were also observed, with E_{onset} slightly shifted to 1.31 V and the reductive wave during the reverse scan greatly diminished, Figure S7. This observation is consistent with oxidation of Cl^- to Cl_2 followed by disproportionation to $HClO/ClO^-$, favored by $\Delta G° = -0.16$ eV at this pH.[12]

Controlled potential electrolysis experiments were conducted at a relatively large surface area GC plate (1.0 cm²) at 1.6 V in 0.1 M HNO_3 (pH 1) with 1 M NaCl and 50 μM Ag(I), Figure 1B. Electrocatalysis was sustained at a stable current density level of ~2 mA/cm². Cl_2 was swept from the reaction solution by a slow Ar purge into a KI/starch aqueous solution, and the amount of Cl_2 produced was determined by iodometric titration. The analytical result gave 110 μmol of Cl_2 over an electrolysis period of 4 h, with a Faradaic efficiency of 71% for Cl_2 production. No significant production of O_2 was observed by an oxygen probe.

Unlike heterogeneous Ag(I)-catalyzed H_2O oxidation in Figures S2−S5, Ag(I)-catalyzed Cl^- oxidation is homogeneous. Heterogeneous catalysis is typically characterized by CV crossover profiles and rising current densities during electrolysis due to the buildup of catalyst on the electrode surface. As shown in Figure 1, these behaviors are not observed for Cl^- oxidation to Cl_2. Moreover, following long-term electrolysis, SEM and XPS show no evidence for precipitation or film formation. At pH 7, the available evidence is also clearly consistent with homogeneous catalysis of Cl^- oxidation by Ag(I).

The appearance of selective Cl^- oxidation in acidic aqueous solutions of μM Ag(I) in competition with H_2O oxidation is remarkable. The selectivity has a mechanistic basis. In H_2O oxidation, O---O bond formation is often the rate-limiting step.[10] Rate enhancements are observed with added proton-acceptor bases,[13] or with intramolecular proton-relay bases[14] arising from O-atom proton transfer in which a H^+ is lost in concert with O---O bond formation, e.g., $Ru^V(O)^{3+}\cdots O(H)H\cdots B^- \rightarrow Ru^{III}-OOH^{2+} + HB$.[13] By contrast, Cl^- oxidation to Cl_2 does not involve net proton transfer and is kinetically favored, even in acidic solution.

From the electrochemical data, the Ce(IV/III) couple is sufficiently oxidizing to drive Ag(I)-catalyzed Cl^- oxidation. As shown in Figures S6 and S8, neither Ag(I) nor its complexes with Cl^- absorb above 250 nm, and UV−visible measurements can monitor the kinetics of Ce(IV) consumption. In these experiments, with a large excess of Cl^- (>100 fold) relative to Ag(I) and Ce(IV), [Cl^-] remained pseudo-first-order over the course of the reaction (see below).

In 0.1 M HNO_3, loss of Ce(IV), monitored at 400 nm, is first-order in Ce(IV), Figure 2A, consistent with eq 5 and the integrated rate law, $\ln([C_0]/[C_t]) = \ln(A_0/A_t) = k_{obs}t$, with A_0 and A_t the absorbance at time 0 and t, respectively. First-order rate constants, k_{obs}, were evaluated from plots of $-\ln(A_t)$ vs t. Figure 2B shows a plot of k_{obs} vs [Ag(I)] from 10 to 80 μM. The linear variation is consistent with a first-order dependence on [Ag(I)], with $k_{obs} = k'[Ag(I)]$, consistent with eq 6a. From the plot of k_{obs} vs [Ag(I)] in Figure 2B, $k' = 27$ M^{-1} s^{-1} at [Cl^-] = 1 M. The linear dependence of the rate law on [Ag(I)] is consistent with the electrochemical result in Figure 1A, inset.

$$\text{rate} = d[Ce(IV)]/dt = k_{obs}[Ce(IV)] \qquad (5)$$

$$d[Ce(IV)]/dt = k'[Ce(IV)][Ag(I)] \qquad (6a)$$

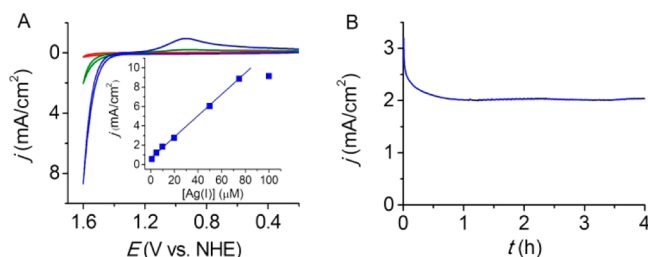$$d[Ce(IV)]/dt = k_o[Ce(IV)][Ag(I)][Cl^-] \qquad (6b)$$

Figure 1. (A) CVs at a GC electrode (0.071 cm²) in 0.1 M HNO_3 (red) and in solutions 1 M in NaCl in 0.1 M HNO_3 without (green) and with (blue) 50 μM Ag(I) at 100 mV/s. Inset: plot of catalytic current vs Ag(I) concentration. (B) Controlled potential electrolysis at a GC plate (1.0 cm²) at 1.6 V in 0.1 M HNO_3 with 1 M added NaCl and 50 μM Ag(I).
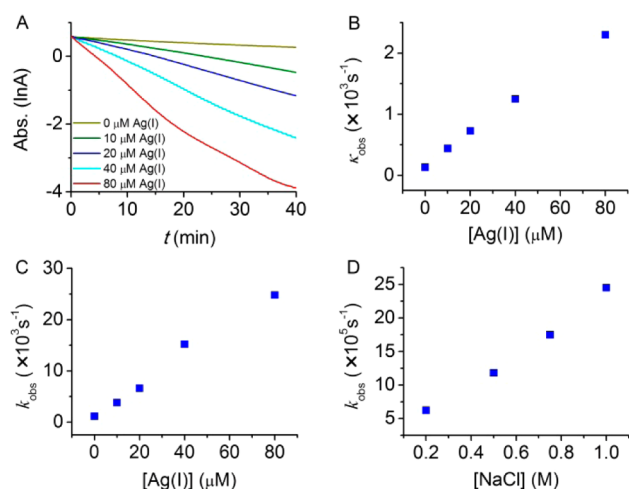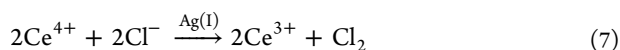
Figure 2. (A) Ce(IV) monitoring at 400 nm with 10 mM added Ce(IV) and 1 M NaCl in 0.1 M HNO$_3$ with increasing amounts of Ag(I). (B) Plot of k_{obs} (from panel A) vs [Ag(I)] in 0.1 M HNO$_3$. (C) Plot of k_{obs} (from Figure S9A) vs [Ag(I)] in 1 M HNO$_3$. (D) Plot of k_{obs} (from Figure S9B) vs [NaCl] with 8 μM Ag(I) in 0.1 M HNO$_3$.

Applying the same analysis to data obtained in 1.0 M HNO$_3$ gives $k' = 272$ M^{-1} s^{-1} at [Cl$^-$] = 1 M, Figures S9A and 2C. The enhanced rate constant under these conditions is presumably due, at least in part, to an enhanced driving force for Ce(IV) oxidation of Ag(I), given the enhanced $E^{\circ\prime}$ value for the Ce(IV/III) couple at the higher acid concentration.[10] This rate constant of Cl$^-$ oxidation by Ce(IV) in 1.0 M HNO$_3$ is ~20 times higher than that of H$_2$O oxidation with polypyridyl Ru complexes under comparable experimental conditions.[10]

The reaction is also first-order in [Cl$^-$], with the complete rate law given in eq 6b. These experiments were conducted at constant [Ag(I)] = 8 μM and [Ce(IV)] = 10 mM in 0.1 M HNO$_3$. As shown in Figures S9B and 2D, k_{obs} varies linearly with [Cl$^-$] from 0.2 to 1 M. From the plot of k_{obs} vs [Cl$^-$], $k' = 2.3 \times 10^{-4}$ M^{-1} s^{-1}, with $k_0 = k'/[Ag(I)] = 29$ M^{-2} s^{-1}.

Sustained catalysis by Ce(IV) as oxidant was investigated by sequential additions of Ce(IV) to a solution 80 μM in Ag(I) and 1 M in NaCl in 0.1 M HNO$_3$ following complete consumption of Ce(IV). As shown in Figure S10, time-dependent absorbance changes are essentially the same for five sequential additions of 10 mM Ce(IV), with a total 625 equiv of Ce(IV) added per Ag(I). After the reaction there was no evidence for particle formation in solution, Figure S11, consistent with a homogeneous catalysis.

Qualitative production of Cl$_2$ was confirmed by positioning wet KI/starch test paper in the headspace of a reaction flask containing 80 μM Ag(I), 10 mM Ce(IV), and 1 M NaCl in 0.1 M HNO$_3$. The test paper turned blue within 3 min; by contrast, there was negligible color change in 30 min without added Ag(I). Quantitative Cl$_2$ analyses by iodometric titration with Cl$_2$ purged into a KI/starch aqueous solution gave 88($\pm$3)% of the expected Cl$_2$ after 55 turnovers per added Ag(I). The results obtained are consistent with stoichiometric Cl$_2$ production and the reaction in eq 7. There was no evidence for O$_2$ production by oxygen measurements.

$$2Ce^{4+} + 2Cl^- \xrightarrow{Ag(I)} 2Ce^{3+} + Cl_2 \qquad (7)$$

There was an unexpected H$_2$O/D$_2$O solvent isotope effect on the rate of Cl$^-$ oxidation. Figure 3A shows that, in D$_2$O as solvent, the rate of Cl$^-$ oxidation in 1 M NaCl in 0.1 M HNO$_3$ was
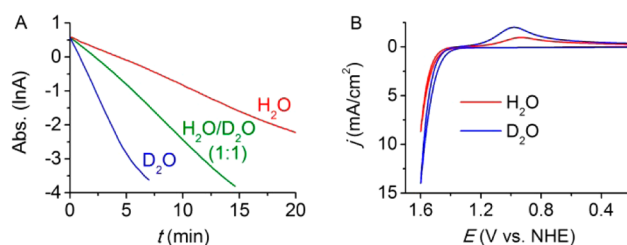

Figure 3. (A) Ce(IV) monitoring at 400 nm with 80 μM Ag(I), 10 mM Ce(IV), and 1 M NaCl in 0.1 M HNO$_3$ with H$_2$O, H$_2$O/D$_2$O (1:1), and D$_2$O as solvents. (B) CVs at a GC electrode (0.071 cm^2) at 100 mV/s with 50 μM Ag(I) and 1 M NaCl in 0.1 M HNO$_3$ with H$_2$O and D$_2$O as solvents.

enhanced, with an inverse kinetic isotope effect of k_{obs}(H$_2$O)/k_{obs}(D$_2$O) = 0.25. A similar result was also obtained by CV, Figure 3B. The origin of the inverse isotope effect is unclear; it may be due to a solvent effect with weaker H-bond interactions between Cl$^-$ and D$_2$O compared to H$_2$O activating Cl$^-$ toward oxidation or from an acid/base pre-equilibrium with a significant inverse isotope effect.[15]

Catalysis of Ce(IV) oxidation of Cl$^-$ to Cl$_2$ is specific to Ag(I) for its specific coordination and redox chemistry, as discussed below. There was no evidence for Cl$^-$ oxidation following addition of 0.5−1 mM Cu(II), Co(II), Ni(II), or Fe(III) to solutions of 10 mM Ce(IV) and 1 M NaCl in 0.1 M HNO$_3$, Figure S12.

Theoretical analysis of Ag(I) catalysis of Cl$^-$ oxidation was done by both density functional theory with the B3LYP functional (DFT) and the coupled-cluster method with single and double excitations (CCSD) (see SI for details). Similar results on geometries and energies were obtained by both methods, although CCSD generally gave lower oxidation potentials and shorter Ag−Cl bond lengths. The DFT results are presented in Scheme 1, and those from CCSD in Figure S13.

Scheme 1. Mechanism of Catalytic Chloride Oxidation to Chlorine by Ag(I) in Concentrated Chloride Solutions Based on DFT Calculations^a
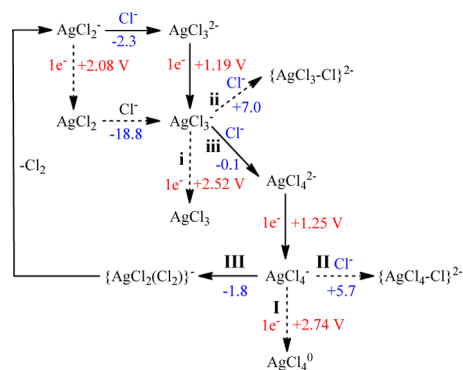
^{a}The values in red are calculated redox potentials (vs NHE). The values in blue are free energy changes (kcal/mol).

Soluble complexes derived from AgCl in aqueous Cl$^-$ solutions have been investigated extensively with two-, three-, and, in rare cases, four-Cl$^-$-coordinated Ag(I) invoked, eq 8.[11] In an early report,[11a] Fritz analyzed available data in the literature to rationalize the thermodynamic parameters associated with formation of Ag(I) complex anions with Cl$^-$. Formation constants (K), defined in eq 9, for Ag complexes in H$_2$O at 25

°C are as follow:[11a] $AgCl^0$, 3.1×10^{-7}; $AgCl_2^-$, 2.5×10^{-5}; $AgCl_3^{2-}$, 2.0×10^{-5}; and $AgCl_4^{3-}$, 7.8×10^{-7}. They point to $AgCl_2^-$ and $AgCl_3^{2-}$ as the dominant species in 1 M NaCl, with no more than 3% $AgCl^0$ and $AgCl_4^{3-}$. There is no evidence for the presence of di-Ag in solution.

$$AgCl(s) + (n-1)Cl^-(aq) \rightleftharpoons AgCl_n^{1-n} \quad (8)$$
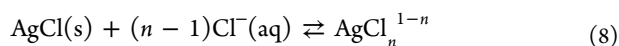
$$K = \left[AgCl_n^{1-n} \right] / \left[Cl^- \right]^n \quad (9)$$

From calculated standard electrode potential ($E°$) values for the Ag(II/I) couples, $AgCl_2^{0/-}$ and $AgCl_3^{-/2-}$, oxidation of $AgCl_2^-$ to $AgCl_2^0$ requires a potential of 2.08 V vs NHE. This value is greatly in excess of $E_{onset} = 1.37$ V measured in the CV experiment, Figure 1A. In contrast, $E°$ for oxidation of $AgCl_3^{2-}$, having a D_{3h} symmetric trigonal-planar geometry, is 1.19 V, comparable to the experimental value. Based on the DFT results, the minimum energy structure for 1e⁻-oxidized $AgCl_3^-$ is T-shaped, with C_{2v} symmetry, Figure S14. Population analysis from the calculations shows 33% (1.29) of the Mulliken spin density (Mulliken atomic charge) on the Ag atom, 35% (−0.59) on the Cl atom along the axis of symmetry, and the rest spread equally on the other two Cl atoms (16% on each, −0.85), Figure S15. The considerable Cl spin densities show that oxidation of $AgCl_3^{2-}$ is delocalized over the metal and Cl⁻ ligands, lowering the Ag(II/I) potential.

Three possible reaction pathways were analyzed for Cl⁻ oxidation by $AgCl_3^-$: (i) further 1e⁻ oxidation to $AgCl_3^0$, which would require an unrealistically high potential of 2.52 V; (ii) Cl⁻ attack on the Cl atom along the axis of symmetry to form an intermediate complex, $\{AgCl_3-Cl\}^{2-}$ while the reaction between Cl⁻ and Cl• free radical to give Cl_2^- is thermodynamically favorable,[16] Cl⁻ attack on the coordinated Cl⁻ is thermodynamically unfavorable by $\Delta G = +7.0$ kcal/mol; and (iii) prior Cl⁻ coordination to $AgCl_3^-$ to form $AgCl_4^{2-}$. Unlike Cl⁻ attack, coordination expansion at Ag(II) is thermodynamically favored by $\Delta G = -0.1$ kcal/mol. $AgCl_4^{2-}$ has a D_{4h} symmetric square-planar geometry with spin densities (atomic charges) of 30% (+1.32) on the Ag atom and 18% (−0.83) on each Cl atom, Figure S15. Further oxidation of $AgCl_4^{2-}$ to $AgCl_4^-$ requires a potential of 1.25 V. The small potential separation between $E°$ values for the $AgCl_3^{-/2-}$ and $AgCl_4^{-/2-}$ couples is a consequence of "redox potential leveling" by Cl⁻ coordination to avoid charge buildup.

Based on the calculations, twice-oxidized $AgCl_4^-$ retains square-planar geometry. The Mulliken atomic charges are +1.71 on the Ag atom and −0.68 on each Cl atom. Three possible pathways for Cl⁻ oxidation by $AgCl_4^-$ were also considered, revealing that (I) oxidation of $AgCl_4^-$ to $AgCl_4^0$ is thermodynamically disfavored, with $E^0 = +2.74$ V; (II) Cl⁻ attack to form $\{AgCl_4-Cl\}^{2-}$ is also unfavorable by $\Delta G = +5.7$ kcal/mol; and (III) formation of the molecular association complex, $\{AgCl_2(Cl_2)\}^-$, is slightly exothermic, with $\Delta G = -1.8$ kcal/mol. Once formed, this intermediate can release Cl_2 which, followed by Cl⁻ coordination, regenerates $AgCl_3^-$ to complete the catalytic cycle.

Our observations are important in demonstrating sustained homogeneous chloride oxidation to chlorine at low overpotentials based on simple Ag(I) in concentrated Cl⁻, perhaps making seawater an appealing substrate in solar fuel energy conversion schemes. It may also serve as an attractive alternative to the conventional DSA electrode for the chlor-alkali industry. Cl⁻ coordination to form $AgCl_2^-$ and $AgCl_3^{2-}$ complex anions in solution avoids precipitation of Ag(I) as AgCl. Cl⁻ coordination also provides access to Ag(II) and Ag(III) by delocalizing the oxidative charges over the Cl⁻ ligands, greatly decreasing the potentials required to reach the higher oxidation states. The simplicity of the system, well-defined mechanistic insight, and requirement for small quantities of Ag(I) for catalysis are appealing and may be of value in electrochemical or photoelectrochemical applications.

■ ASSOCIATED CONTENT

Ⓢ Supporting Information

Additional information as noted in the text. This material is available free of charge via the Internet at http://pubs.acs.org.

■ AUTHOR INFORMATION

Corresponding Authors
*zfchen@tongji.edu.cn
*ccchen@iccas.ac.cn

Notes
The authors declare no competing financial interest.

■ ACKNOWLEDGMENTS

■ REFERENCES

(1) Cook, T. R.; Dogutan, D. K.; Peece, S. Y.; Surendranath, Y.; Teets, T. S.; Nocera, D. G. *Chem. Rev.* **2010**, *110*, 6474.

(2) (a) Lakshmanan, S.; Murugesan, T. *Clean Technol. Environ. Policy* **2014**, *16*, 225. (b) Exner, K. S.; Anton, J.; Jacob, T.; Over, H. *Angew. Chem., Int. Ed.* **2014**, *53*, 11032.

(3) Zeradjanin, A. R.; Schilling, T.; Seisel, S.; Bron, M.; Schuhmann, W. *Anal. Chem.* **2011**, *83*, 7645.

(4) Ellis, C. D.; Gilbert, J. A.; Murphy, W. R.; Meyer, T. J. *J. Am. Chem. Soc.* **1983**, *105*, 4842.

(5) Ferrere, S.; Gregg, B. A. *J. Chem. Soc., Faraday Trans.* **1998**, *94*, 2827.

(6) Aoki, K.; Chen, H.; Chen, J. *Electrochem. Commun.* **2007**, *9*, 2304.

(7) (a) Lehmani, A.; Turq, P.; Simonin, J. P. *J. Electrochem. Soc.* **1996**, *143*, 1860. (b) Bringmann, J.; Ebert, K.; Galla, U.; Schmieder, H. *J. Appl. Electrochem.* **1995**, *25*, 846.

(8) Mentasti, E.; Baiocchi, C.; Coe, J. S. *Coord. Chem. Rev.* **1984**, *54*, 131.

(9) Wang, W.; Zhao, Q.; Dong, J.; Li, J. *Int. J. Hydrogen Energy* **2011**, *36*, 7374.

(10) Concepcion, J. J.; Tsai, M.-K.; Muckerman, J. T.; Meyer, T. J. *J. Am. Chem. Soc.* **2010**, *132*, 1545.

(11) (a) Fritz, J. J. *J. Solution Chem.* **1985**, *14*, 865 and references therein. (b) Muller-Rosing, H. C.; Schulz, A.; Hargittai, M. *J. Am. Chem. Soc.* **2005**, *127*, 8133.

(12) Wang, T. X.; Margerum, D. W. *Inorg. Chem.* **1994**, *33*, 1050.

(13) Chen, Z.; Concepcion, J. J.; Hu, X.; Yang, W.; Hoertz, P. G.; Meyer, T. J. *Proc. Natl. Acad. Sci. U.S.A.* **2010**, *107*, 7225.

(14) (a) Privalov, T.; Åkermark, B.; Sun, L. *Chem.—Eur. J.* **2011**, *17*, 8313. (b) Boyer, J. L.; Polyansky, D. E.; Szalda, D. J.; Zong, R.; Thummel, R. P.; Fujita, E. *Angew. Chem., Int. Ed.* **2011**, *50*, 12600.

(15) Huynh, M. H. V.; Meyer, T. J. *Chem. Rev.* **2007**, *107*, 5004.

(16) Mártire, D. O.; Rosso, J. A.; Bertolotti, S.; Le Roux, G. C.; Braun, A. M.; Gonzalez, M. C. *J. Phys. Chem. A* **2001**, *105*, 5385.